



# Synthesis of Silver Nanoparticles Using Extracts from Yerba Mate (*Ilex paraguariensis*) Wastes

Romina A. Arreche<sup>1</sup> · Gabriela Montes de Oca-Vásquez<sup>2</sup> · Jose R. Vega-Baudrit<sup>2</sup> · Patricia G. Vázquez<sup>1</sup>

Received: 14 November 2017 / Accepted: 25 June 2018  
© Springer Nature B.V. 2018

## Abstract

Synthesis of metallic nanoparticles by an eco-friendly and sustainable process is an important target to be developed in nanotechnology area. In the present work, two different commercial brands of yerba mate from Argentina and their wastes (PYM and TYM samples) were used for the preparation of aqueous extracts, in order to synthesize silver nanoparticles at room temperature (25 °C). The silver nanoparticles obtained were spherical, hexagonal and, triangular in shape with the average particle size of 50 nm and, shows a surface plasmon peak around 460 nm. The antimicrobial activity of the silver nanoparticles obtained with the extracts from yerba mate wastes was evaluated against *E. coli* and *S. aureus*. The minimum inhibitory concentrations required for *E. coli* were 7.66 and 17.66  $\mu\text{g ml}^{-1}$  using the treatment T2YE and P2YE, respectively and, for *S. aureus* were 23.25 and 50.60  $\mu\text{g ml}^{-1}$  for the treatment T2YE and P2YE, respectively. The study suggests that polyphenols present in *I. paraguariensis* leaf extract act as reducing agent and stabilizer of the nanoparticles.

## Graphical Abstract



**Keywords** Yerba mate · Wastes · Silver nanoparticles · Eco-friendly synthesis · Transmission electronic microscopy · Antibacterial activity

## Statement of Novelty

In this article, we report an eco-friendly and sustainable way to synthesized silver nanoparticles with antimicrobial properties. Yerba mate wastes have no commercial application for human consumption; therefore recycling their wastes is an important task to be considered. Also, this paper has original data due to there is no mention in bibliography about the synthesis of nanoparticles using yerba mate extracts.

✉ Romina A. Arreche  
arrecheromina@gmail.com

<sup>1</sup> CINDECA – Centro de Investigación y Desarrollo en Ciencias Aplicadas, “Dr. Jorge J. Ronco”, CONICET – CIC – UNLP, 1900 La Plata, Buenos Aires, Argentina

<sup>2</sup> LANOTEC – National Laboratory of Nanotechnology, Centro Nacional de Alta Tecnología (CeNAT – CONARE), San Jose, Costa Rica

## Introduction

Yerba mate is a popular tea-like beverage widely consumed in Argentina and a large amount of wastes are disposed daily after the “mate consumption”. Commercial yerba is produced in South American countries, such as Argentina, Brazil, Chile, Paraguay, Peru and Uruguay [1], and is obtained from the leaves and stems of *Ilex paraguariensis* after their processing, milling and packaging. Argentina is one of most important exporters of yerba mate and is second behind Uruguay for highest per capita consumption [2]. It is expected an increasing consumption over time around the world due to the well know information about their potential health benefits—antimicrobial, antioxidant, anti-diabetic, digestive improvement, stimulant, and cardiovascular properties [3–5]. Statistical data registered by the National Institute of Yerba Mate (INYM) revealed that during the period of January to July of 2017 an amount of 551,743,283 tons of yerba mate was produced, and this value is the closest index to the behavior of yerba mate in the market [6].

Yerba mate contains various substances biochemically active, responsible of their several properties, such as polyphenols, xanthines, alkaloids, flavonoids, vitamins and several minerals [7, 8]. The yerba mate infusion is prepared bringing together the yerba with water at 70 °C in a recipient called “mate”, showing the use of higher temperatures principally change in organoleptic properties. Bragança et al. [9] evaluated the composition of trace elements in yerba mate infusions of three different commercially available trademarks of *I. paraguariensis* by atomic absorption and, the results showed that the extraction of trace elements from mate (cadmium, lead, copper, zinc, aluminum, iron, chromium, manganese, molybdenum and silver) is not proportional to heat of treatment, probably because of the weak binding of metal ions to the substrate.

Several studies are reported in the literature focused on the synthesis of metallic nanoparticles using natural leaf extracts [10–15]. However, there is no mention about the synthesis of nanoparticles using yerba mate extracts.

Among the different applications of the silver nanoparticles (AgNPs) [16–18], their use as antimicrobial is one of the most interesting, and they have been used in medical devices [19], for disinfection in wastewater treatment plants [20], in textile fabrics [21], paints [22], among others [23].

The aim of this study was to synthesize AgNPs from yerba mate extracts, in a simply way and using a green method. Two brands commercially available of *I. paraguariensis* were evaluated, simulating the popular mode of preparation. The influences of different concentration of yerba mate extract, different metal ion concentration

and different reaction time on the synthesis of nanoparticles were evaluated. The synthesized nanoparticles were characterized using UV–Vis spectroscopy, zeta potential, dynamic light scattering (DLS), atomic force microscopy (AFM), Fourier transform infrared spectroscopy (FT-IR) and transmission electron microscopy (TEM). In addition, the antimicrobial properties of the silver nanoparticles synthesized by yerba mate extracts were also investigated.

## Materials and Methods

### Preparation of Yerba Mate Extracts

Two different commercial brands of yerba mate from Corrientes, Argentina, were used for the preparation of the extracts (PYM and TYM samples). Yerba was grounded in order to reduce the size of the leaf and then 10 g of the obtained solid were weighted and added to 100 ml of Milli-Q water in a flask and heated at 70 °C for 30 min. Then, the extract was centrifuged at 5000 rpm for 15 min, the liquid extract was filtered through Whatman No. 1 filter paper and stored at 4 °C. Two liquid extracts were obtained in this first step, P1YE and T1YE, respectively. The solid extract was reused for a second extraction, simulating the waste disposed after the mate consumption. This solid was added to 100 ml in a flask and heated at 70 °C for 30 min and then centrifuged at 5000 rpm for 15 min. Finally, the liquid extract was filtered through a Whatman No. 1 filter paper and storage at 4 °C, obtaining second extracts, P2YE and T2YE.

### Synthesis of Silver Nanoparticles

For the synthesis of AgNPs, a solution 1 mM of silver nitrate ( $\text{AgNO}_3$ , J.T.Baker) was prepared in an erlenmeyer flask and then, an aliquot of 20 ml was mixed with 2 ml (dilution 1:10) and 400  $\mu\text{l}$  (dilution 1:50) of the aqueous extracts of *Ilex paraguariensis* to evaluate the influence of different concentration of yerba mate extract on the nanoparticles formation. A magnetic stirrer at 1000 rpm was used and the solution was kept at 25 °C for 24 h under darkness. All experiments were carried out in triplicate. The different reaction times on the synthesis of nanoparticles were evaluated and the formed nanoparticles were further characterized.

### Characterization of Silver Nanoparticles

The synthesized nanoparticles were characterized using different techniques. Ultraviolet visible (UV–Vis) spectroscopy was used to measure the reduction of silver ions and the growth of AgNPs with time. The spectral analysis was done using a Shimadzu spectrophotometer (UV-1800) from 200 to 900 nm. Particle size measurement by dynamic light

scattering and zeta potential of silver nanoparticles were carried out by means of laser diffractometry, using a Zetasizer Nano ZS90 (Malvern Instruments). Measurements were acquired in Milli-Q distilled water as dispersant at 25 °C and at a scattering angle of 90° ( $n + 10$ ). Transmission electron microscopy (TEM) of the purified samples of AgNPs were prepared by drop casting 5  $\mu$ l of the reaction mixtures over carbon-coated copper grids, allowing the samples to dry in a desiccator for 16 h. TEM measurements were performed on a JEOL (model JEM 2011) instrument, operated at an accelerating voltage of 120 kV. For a detailed morphology and size of the nanoparticles AFM was employed. Before the analysis, the nanoparticles were purified carrying out the next procedure twice: the nanoparticles were centrifuged with 30% isopropanol at 13,000 rpm for 30 min at 4 °C and the pellet obtained was resuspended in 1.5 ml of Milli Q distilled water. The nanoparticles were redispersed in an ultrasonic bath for 15 min and finally, were sonicated in a GEX 130 Cole-Palmer sonicator for 4 min with a 6 mm titanium probe at 35% amplitude. The purified silver nanoparticles were visualized with an Asylum Research, MFP-3DTM AFM. A drop of AgNPs solution was deposited onto a mica substrate and was allowed to air dry for 24 h. Samples were analyzed using tapping mode AFM using 10 mm silicon nitride probe. The height data was collected at a scanning frequency of 1 Hz. WsxM software (4.0 Develop 8.1, Nanotec Electronica, S.L., Spain) was used for the AFM analysis. In order to determine the main functional groups on the yerba mate extracts, FTIR analysis was carried out using a FTIR spectrophotometer (Nicolet 6700, Thermo Scientific). The samples were lyophilized and analyzed.

### Antimicrobial Activity of Silver Nanoparticles

Representative Gram positive and Gram negative microorganisms (*Staphylococcus aureus* ATCC 25923 and *Escherichia coli* ATCC 25922) were used to evaluate the antibacterial activity of the prepared AgNPs. The determination of minimum inhibitory concentration (MIC) was performed by the Resazurin microtitre assay (REMA) [24]. A bacterial suspension of each bacterium was centrifuged at 3500 rpm for 5 min and the pellets were suspended in saline solution 0.85% m/v NaCl. Then  $5 \times 10^4$  UFC/well of test microorganisms were added to 96-well microtiter plates and the final volume in each well was made up to 100  $\mu$ l. AgNPs were then added in increasing concentrations, and to test for cell viability, 10  $\mu$ l of a 0.01% (m/v) resazurin solution was added to each well. The plates were then incubated at 30 °C for 24 h. After the incubation period the presence of viable microorganisms in each well was estimated by a change in color from blue to a bright pink. All experiments were done in triplicate and averages of the MIC values were reported.

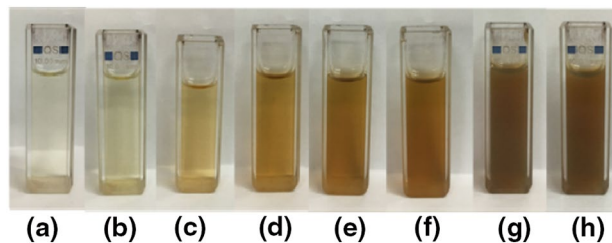


**Fig. 1** Color change during the synthesis of silver nanoparticles after **a** 30 min, **b** 1 h, **c** 2 h, **d** 3 h, **e** 4 h, **f** 5 h, **g** 23 h and **h** 24 h with the dilution 1:10 (1:10 P2YE). (Color figure online)

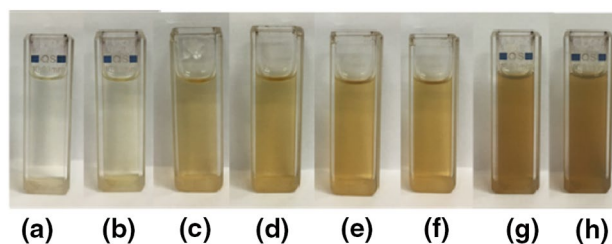


**Fig. 2** Color change during the synthesis of silver nanoparticles after **a** 30 min, **b** 1 h, **c** 2 h, **d** 3 h, **e** 4 h, **f** 5 h, **g** 23 h and **h** 24 h with the dilution 1:50 (1:50 P2YE). (Color figure online)

## Results and Discussion

### Synthesis and Characterization of Silver Nanoparticles

The effect of the concentration of the yerba mate extract (YE) on the nanoparticles formation was studied at 25 °C and, a comparison between different brands of yerba mate was carried out. The nanoparticles formation was evidenced by the appearance of significant brown color of the solution (Figs. 1, 2). Once the nitrate solution was added to the YE, a gradual color change was observed, first a yellow solution was generated by the addition of the extract, and then the brown color was maintained over-time. No differences were observed among the final color of the different brands under the same conditions, but dark brown colors were observed at a dilution 1:10 whereas light brown color were reached at a dilution of 1:50 after 24 h of reaction.

UV–Vis spectroscopy is a useful tool for monitoring the reduction of the silver ions and the nanoparticles formation. It is well known that the optical absorption spectrum of metal nanoparticles are dominated by surface plasmon resonances (SPR) that shift to longer wavelengths with increasing particle size [25]. Also, it is well recognized that the width of each plasmon is related to the size

distribution of the nanoparticles [26]. It is expected that spherical particles show only a single SPR band in the absorption spectrum, whereas irregular particles, such as triangular or square shapes could give rise to two or more SPR bands [27]. The absorption spectrums of the silver nanoparticles at different times for T1YE and P1YE (dilution 1:50) and T2YE and P2YE (dilution 1:10) are presented in Figs. 3 and 4, respectively. All samples showed the characteristic surface plasmon of silver nanoparticles, and an increase of the intensity in the range of 400–500 nm was observed with increasing time. This increase of the peaks intensity indicates that the concentration of silver nanoparticles increases, as a result of reduction of silver ions present in the aqueous solution [28]. A constant maximum between 433 and 450 nm after 24 h was observed for all the samples, indicating a complete formation of nanoparticles and the presence of spherical or roughly spherical

AgNPs. The obtained UV–Vis absorption spectra clearly indicate the successful reduction of Ag into nanoparticles using not only yerba mate leaf extracts but also the wastes after its consumption.

In order to recognize the surface charge, the zeta potential of AgNPs produced was analyzed. Table 1 presents sizes and zeta potential values for all the samples and Fig. 5 shows the DLS size distribution image of AgNPs. From the results showed in Table 1, the calculated average particle size distribution of AgNPs is around 34–38 nm for the first extracts, and 35–53 nm for the second extracts, showing a little increase in particles sizes with yerba mate reused.

Generally, nanoparticles that exhibit zeta potential values less than  $\pm 20$  mV are considered unstable and will result in precipitation of particles from solution, whereas nanoparticles with zeta potential values higher than this value are considered as stable [29, 30]. In this study, zeta potential values

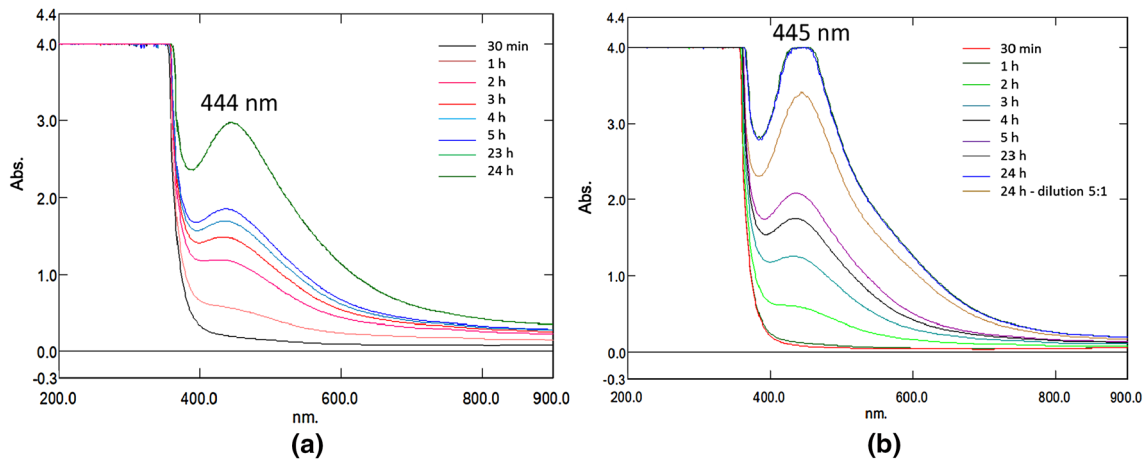


**Fig. 3** UV–Vis absorption spectrum of the AgNPs prepared from **a** T1YE and **b** P1YE (dilution 1:50)

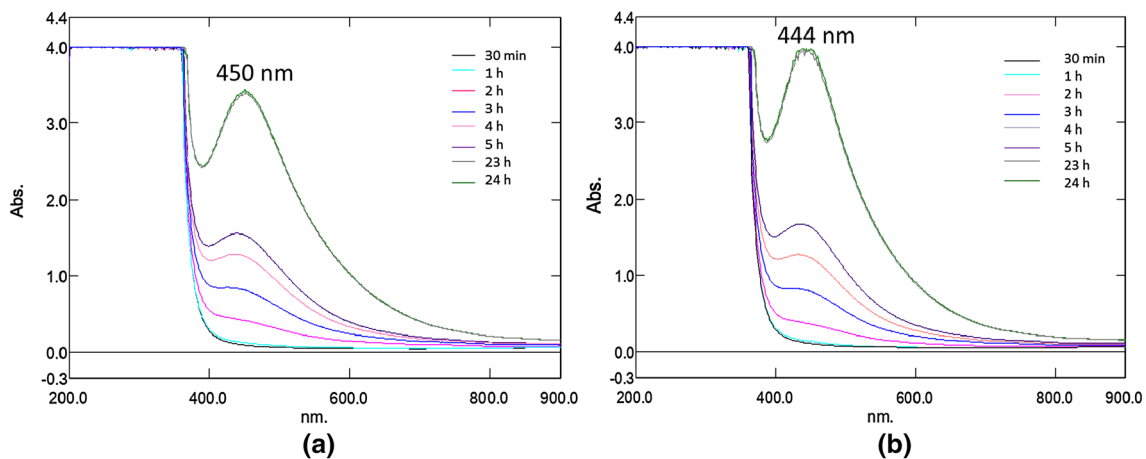


**Fig. 4** UV–Vis absorption spectrum of the AgNPs prepared from **a** T2YE and **b** P2YE (dilution 1:10)

**Table 1** Size and zeta potential values for first and second yerba mate extracts

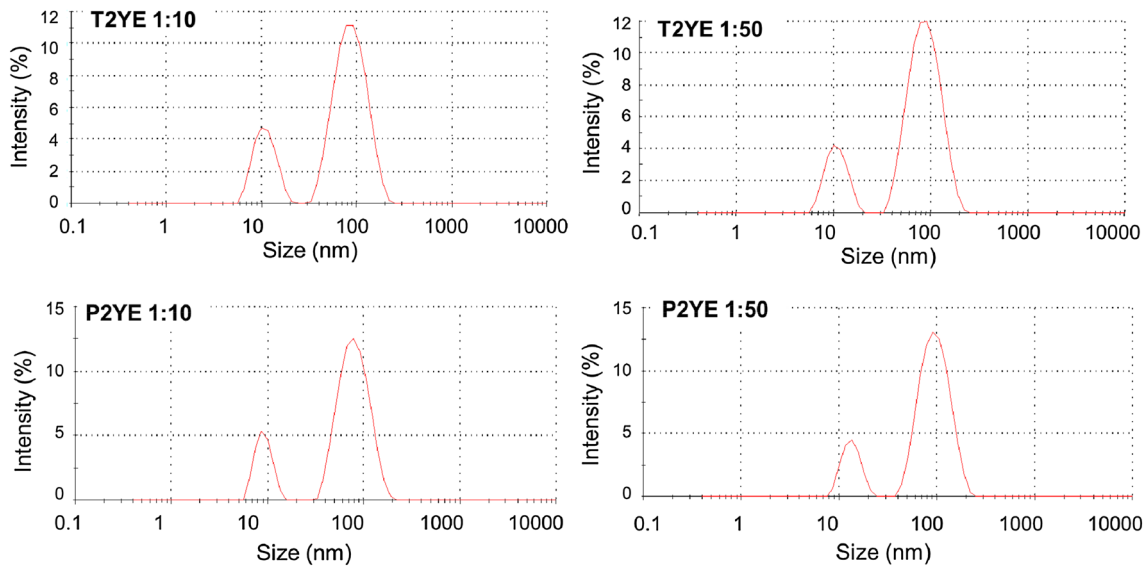
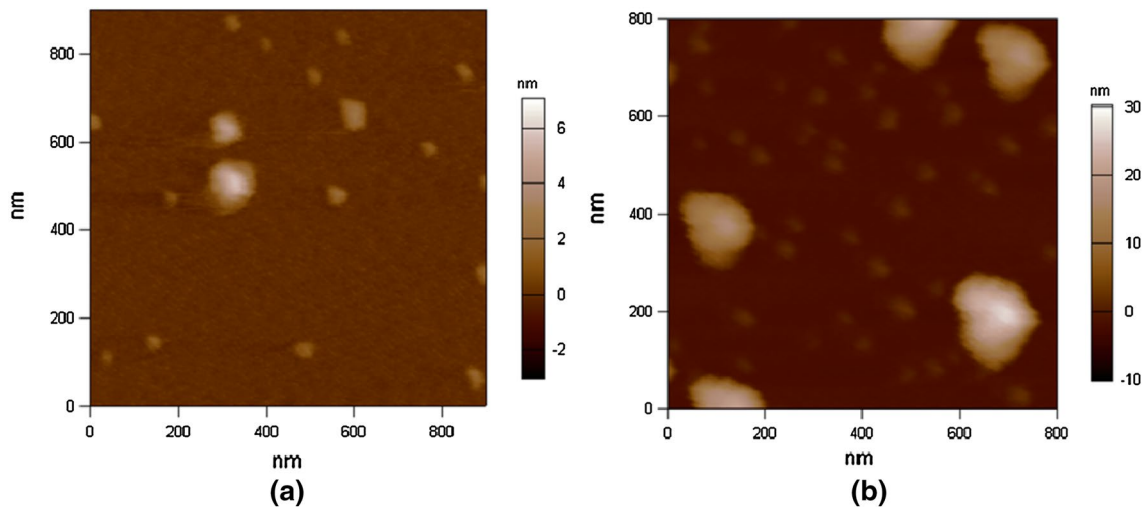
Treatment	Size (nm)	PDL	Zeta potential (mV)
T1YE 1:10	34.60	0.608	$-18.37 \pm 9.94$
T1YE 1:50	36.67	0.595	$-18.75 \pm 12.97$
T2YE 1:10	39.81	0.560	$-19.84 \pm 12.04$
T2YE 1:50	44.86	0.561	$-25.40 \pm 11.74$
P1YE 1:10	33.75	0.610	$-17.38 \pm 10.84$
P1YE 1:50	38.81	0.570	$-19.36 \pm 11.31$
P2YE 1:10	35.04	0.586	$-20.93 \pm 12.88$
P2YE 1:50	53.58	0.519	$-21.47 \pm 8.73$

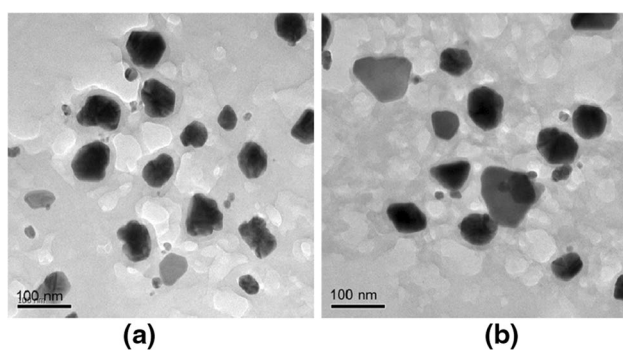
of AgNPs were between  $-17$  and  $-25$  mV for both extracts, indicating the stability of silver nanoparticles suspensions.

Figure 5 shows the size distribution of AgNPs synthesized with the second extracts at different dilutions. The particles are of 10 and 80 nm average diameter with a narrow size distribution.

Figure 6 shows the topographical image of irregular silver nanoparticles synthesized using YE extracts.

Figure 7 shows the TEM images of AgNPs obtained with second extracts of yerba mate and AgNO<sub>3</sub> solution (dilution 1:50). Figure 7a, b reveals that nanoparticles are surrounded by a thin layer of organic material, being this a particular

**Fig. 5** DLS size distribution of AgNPs synthesized with the second extracts at different dilutions**Fig. 6** AFM images of silver nanoparticles synthesized using second extracts of commercial yerba mate, **a** T2YE and **b** P2YE, dilution 1:10



**Fig. 7** TEM images of AgNPs synthesized using second extracts, **a** T2YE and **b** P2TE at a dilution of 1:50

characteristic of AgNPs prepared using plant extracts. In general, the nanoparticles synthesized have spherical shapes but triangular, hexagonal and square particles were also observed (Fig. 8). According to El-Zahry et al. [31], triangular NPs show bands by UV–Vis at 344 and 600 nm and hexagonal NPs shows two bands at about 416 and 650 nm. Instead various peaks, we have obtained a single band at about 450 nm, therefore it is probably that spherical particles were mostly synthesized. The particle size of the silver nanoparticles synthesized was found to be around 10 and 80 nm, in accordance with DLS results.

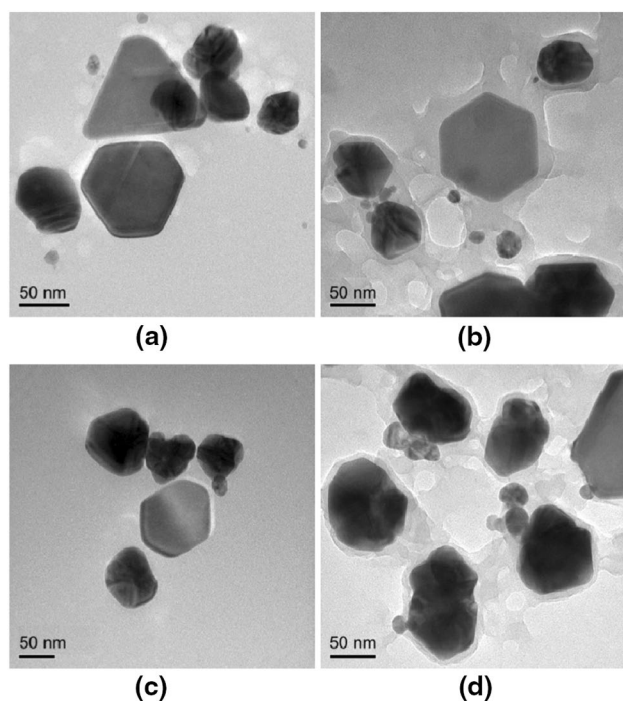


**Fig. 8** TEM images of AgNPs synthesized using second extracts, T2YE **a** dilution 1:10, **b** dilution 1:50 and, P2TE, **c** dilution 1:10 and **d** dilution 1:50

Previous studies have been conducted to determine the bioactive and chemical composition of *Ilex paraguariensis* [7, 32, 33]. According to Bastos et al. [34], yerba mate possesses numerous active compounds in their composition. They determined that the major active phytochemicals present in commercial yerba mate are polyphenols and xantines, such as caffeic acid, caffeine, caffeoyl derivatives, chlorogenic acid, quercetin, rutin, theobromine, among other. Additionally, Isolabella et al. [35] determined the composition of yerba mate during the obtaining process and after a comparative analysis they indicated that those obtained after the drying and aging processes possessed the higher content of biologically active principles, like total caffeoyl derivatives, caffeine, theobromine and rutin, compared with green leaves.

For the characterization and identification of the molecules responsible for the AgNPs synthesis, FTIR analysis was carried out (Fig. 9).

The spectra of YE shows the characteristic bands of typical polyphenols. A broadband centered around  $3370\text{ cm}^{-1}$  is assigned to the stretching modes of O–H groups and to the hydroxyl groups involved in an intermolecular hydrogen bond [36], present in compounds such as chlorogenic acid, saponins and others. The band observed in the region from  $3000$  to  $2800\text{ cm}^{-1}$  is assigned to a stretching vibration of aliphatic CH, CH<sub>2</sub> and CH<sub>3</sub> groups, while that in the region from  $1800$  to  $1500\text{ cm}^{-1}$  is due to the carbonyl group of esters, amides, acids and other compounds such as xanthines and saponins, which are present in the yerba mate [37]. The bands observed in the region from  $1500$  to  $1250\text{ cm}^{-1}$  and those in the regions ranging from  $1300$  to  $1000\text{ cm}^{-1}$  are due the scissor vibration of CH<sub>3</sub> and CH<sub>2</sub> and, the stretching vibration of the C–O bonds, respectively [37].

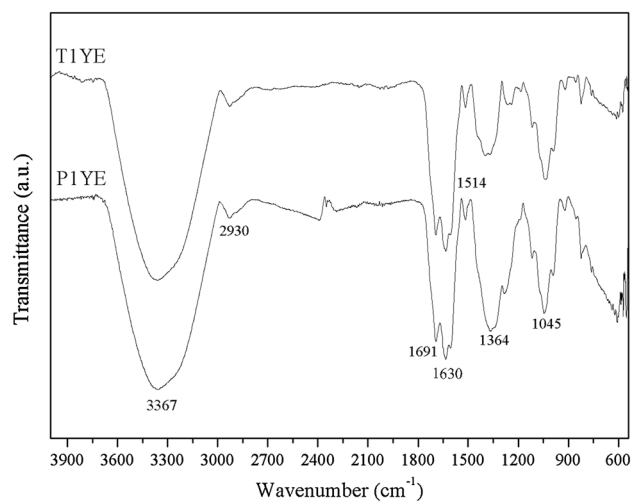


**Fig. 9** FT-IR spectra of lyophilized yerba mate extract, T1YE and P1YE (dilution 1:50)

**Table 2** Minimum inhibitory concentration ( $\mu\text{g ml}^{-1}$ ) of the synthesized AgNPs against *E. coli* and *S. aureus*

Bacterium	Treatments	
	T2YE (1:10)	P2YE (1:10)
<i>Escherichia coli</i>	7.66 <sup>a</sup>	17.66 <sup>a,b</sup>
<i>Staphylococcus aureus</i>	23.25 <sup>b,c</sup>	50.60 <sup>c</sup>

Values with the same letter do not show significant statistical difference

These compounds probably play a key role for the reduction of silver ions and the formation of corresponding nanoparticles, also many studies about nanoparticles syntheses by natural sources support this mechanism [38, 39]. However, particularly the compounds responsible for the reduction and stabilization of the nanoparticles in yerba mate extracts are to be defined in future studies.

### Antimicrobial Activity of Nanoparticles

Due to the result of the synthesis of the nanoparticles, we tested the antibacterial activity using the treatment P2YE y T2YE, dilution 1:10. The synthesized AgNPs displayed antimicrobial activity toward the tested pathogenic strains of *E. coli* and *S. aureus*. The minimum inhibitory concentration required for *E. coli* was  $7.66 \mu\text{g ml}^{-1}$  using the treatment T2YE and  $17.66 \mu\text{g ml}^{-1}$  using the P2YE treatment. The MIC obtained for *S. aureus* was 23.25 and  $50.60 \mu\text{g ml}^{-1}$  for the T2YE and P2YE treatments, respectively. The method used showed the highest antimicrobial activity against *E. coli* than *S. aureus* (Table 2).

The enhanced ability of the synthesized AgNPs to inhibit the growth of *E. coli* and *S. aureus*, confirmed that the nanoparticles obtained from *Ilex paraguariensis* extracts had a great potential to be used as antimicrobial agents against pathogenic microorganisms. The antibacterial activity of nanoparticles is determined by their size, shape, and concentration, and depends of the type of bacteria. Large nanoparticles allow large surface areas to contact bacterial cells, meaning that smaller particles will potentially have higher percentages of interactions relative to larger particles [40]. We determined that the synthesized nanoparticles using the treatment T2YE and P2YE shows similar morphology and size, however we found that the AgNPs had more antibacterial activity against *E. coli* than *S. aureus*, this could be due to differences between the structure of the wall cell of Gram negative and Gram positive bacteria. The cell wall of *E. coli* is composed of a thin layer of peptidoglycan, consisting of linear polysaccharide chains crosslinked by short peptides ( $\sim 7\text{--}8 \text{ nm}$ ). Thus forming thinner structures leading to an easy penetration of SNPs as compared to that of *S. aureus*,

where the cell wall possesses thick layer of peptidoglycan ( $\sim 20\text{--}80 \text{ nm}$ ) [41, 42].

The results of the major antibacterial activities against *E. coli* than *S. aureus*, are in concordance with those reported earlier by Kim et al. [19], Agnihotri et al. [43], Ibrahim et al. [44] and Rasulov et al. [42].

Despite of the mechanism of the antibacterial effect of silver nanoparticles against bacteria is not completely known, some studies have determined that AgNPs may cause damage to the membrane and wall structure, which can disturb important functions such as permeability, osmoregulation, electron transport and respiration [44, 45]. Also, have been attributed to the inhibitory activity of silver nanoparticles on the respiratory enzymes (cytochrome oxidases, malate dehydrogenase and succinate dehydrogenase) [45]. Silver has a greater affinity to react with sulfur- or phosphorus-containing biomolecules in the cell. Thus, sulfur-containing proteins in the membrane or inside the cells and phosphorus-containing elements like DNA are likely to be the preferential sites for silver nanoparticle binding. On the other hand, it has been determined that AgNPs produce degradation in the chromosomal DNA of *B. subtilis* cells. In addition, it increases the activity of reactive oxygen species (ROS) [41].

### Conclusions

Silver nanoparticles with different shapes were obtained at room temperature using water-soluble yerba mate extracts prepared from commercial yerba mate. When yerba mate extracts were mixed with  $\text{AgNO}_3$  solution, the pale yellow color of aqueous extract changed to brownish color indicating the formation of silver nanoparticles. Polyphenols present in *I. paraguariensis* leaf extract might act as reducing agent and stabilizer of the nanoparticles. Moreover, the synthesized silver nanoparticles presented an excellent antimicrobial activity against the evaluated pathogenic microorganisms. Yerba mate wastes have no commercial application for human consumption; therefore recycling their wastes is an important task to be considered. This method appears to be an ecofriendly and low-cost way for producing silver nanoparticles with antimicrobial properties.

**Acknowledgements** The authors would like to express their thanks for the financial support provided by Laboratorio Nacional de Nanotecnología (LANOTEC), Centro Nacional de Alta Tecnología (CeNAT-CONARE), POLIUNA-UNIVERSIDAD NACIONAL de Costa Rica, National Scientific and Technical Research Council (CONICET) and National University of La Plata (UNLP). They also thank to Reynaldo Pereira for TEM micrographs, Universidad Nacional for the Dynamic light scattering (DLS) and Zeta potential analysis, and Yendry Corrales Ureña for AFM images.

## References

- Grigioni, G., Carduza, F., Irurueta, M., Pensel, N.: Flavour characteristics of *Ilex paraguariensis* infusion, a typical Argentine product, assessed by sensory evaluation and electronic nose. *J. Sci. Food Agric.* **84**, 427–432 (2004). <https://doi.org/10.1002/jsfa.1670>
- Bracesco, N., Sanchez, A.G., Contreras, V., Menini, T., Gugliucci, A.: Recent advances on *Ilex paraguariensis* research: minireview. *J. Ethnopharmacol.* **136**, 378–384 (2011). <https://doi.org/10.1016/j.jep.2010.06.032>
- Heck, C.I., De Mejia, E.G.: Yerba mate tea (*Ilex paraguariensis*): a comprehensive review on chemistry, health implications, and technological considerations. *J. Food Sci.* (2007). <https://doi.org/10.1111/j.1750-3841.2007.00535.x>
- Filip, R., Sebastian, T., Ferraro, G., Anesini, C.: Effect of *Ilex* extracts and isolated compounds on peroxidase secretion of rat submandibular glands. *Food Chem. Toxicol.* **45**, 649–655 (2007). <https://doi.org/10.1016/j.fct.2006.10.014>
- Conforti, A.S., Gallo, M.E., Saraví, F.D.: Yerba mate (*Ilex paraguariensis*) consumption is associated with higher bone mineral density in postmenopausal women. *Bone.* **50**, 9–13 (2012). <https://doi.org/10.1016/j.bone.2011.08.029>
- Instituto Nacional de la Yerba Mate, Instituto Nacional de la Yerba Mate (2016). <http://yerbamateargentina.org.ar/>
- Burris, K.P., Harte, F.M., Davidson, P.M., Neal Stewart, C. Jr., Zivanovic, S.: Composition and bioactive properties of yerba mate (*Ilex paraguariensis* A. St.-Hil.): a review. *Chil. J. Agric. Res.* **72**, 268–275 (2012). <https://doi.org/10.4067/S0718-58392012000200016>
- Filip, R., López, P., Giberti, G., Coussio, J., Ferraro, G.: Phenolic compounds in seven South American *Ilex* species. *Fito-terapia.* **72**, 774–778 (2001). [https://doi.org/10.1016/S0367-326X\(01\)00331-8](https://doi.org/10.1016/S0367-326X(01)00331-8)
- Bragança, V.L.C., Melnikov, P., Zanoni, L.Z.: Trace elements in different brands of yerba mate tea. *Biol. Trace Elem. Res.* **144**, 1197–1204 (2011). <https://doi.org/10.1007/s12011-011-9056-3>
- Niraimathi, K.L., Sudha, V., Lavanya, R., Brindha, P.: Bio-synthesis of silver nanoparticles using *Alternanthera sessilis* (Linn.) extract and their antimicrobial, antioxidant activities. *Colloids Surf. B* **102**, 288–291 (2013). <https://doi.org/10.1016/j.colsurfb.2012.08.041>
- Bindhu, M.R., Umadevi, M.: Synthesis of monodispersed silver nanoparticles using *Hibiscus cannabinus* leaf extract and its antimicrobial activity. *Spectrochim Acta A* **101**, 184–190 (2013). <https://doi.org/10.1016/j.saa.2012.09.031>
- Mittal, A.K., Chisti, Y., Banerjee, U.C.: Synthesis of metallic nanoparticles using plant extracts. *Biotechnol. Adv.* **31**, 346–356 (2013). <https://doi.org/10.1016/j.biotechadv.2013.01.003>
- Hebbalalu, D., Lalley, J., Nadagouda, M.N., Varma, R.S.: Greener techniques for the synthesis of silver nanoparticles using plant extracts, enzymes, bacteria, biodegradable polymers, and microwaves. *ACS Sustain. Chem. Eng.* **1**, 703–712 (2013). <https://doi.org/10.1021/sc4000362>
- Kharissova, O.V., Dias, H.V.R., Kharisov, B.I., Pérez, B.O., Pérez, V.M.J.: The greener synthesis of nanoparticles. *Trends Biotechnol.* **31**, 240–248 (2013). <https://doi.org/10.1016/j.tibtech.2013.01.003>
- Ahmed, S., Ahmad, M., Swami, B.L., Ikram, S.: A review on plants extract mediated synthesis of silver nanoparticles for antimicrobial applications: a green expertise. *J. Adv. Res.* **7**, 17–28 (2016). <https://doi.org/10.1016/j.jare.2015.02.007>
- Patel, A.C., Li, S., Wang, C., Zhang, W., Wei, Y.: Electrospinning of porous silica nanofibers containing silver nanoparticles for catalytic applications. *Chem. Mater.* **19**, 1231–1238 (2007). <https://doi.org/10.1021/cm061331z>
- Abou El-Nour, K.M.M., Eftaiha, A., Al-Warthan, A., Ammar, R.A.A.: Synthesis and applications of silver nanoparticles. *Arab. J. Chem.* **3**, 135–140 (2010). <https://doi.org/10.1016/j.arabjc.2010.04.008>
- Rauwel, E., Simón-Gracia, L., Guha, M., Rauwel, P., Kuunal, S., Wragg, D.: Silver metal nanoparticles study for biomedical and green house applications. *IOP Conf. Ser. Mater. Sci. Eng.* **175**, 11001 (2016). <https://doi.org/10.1088/1742-6596/755/1/011001>
- Kim, J.S., Kuk, E., Yu, K.N., Kim, J.H., Park, S.J., Lee, H.J., Kim, S.H., Park, Y.K., Park, Y.H., Hwang, C.Y., Kim, Y.K., Lee, Y.S., Jeong, D.H., Cho, M.H.: Antimicrobial effects of silver nanoparticles. *Nanomed. Nanotechnol. Biol. Med.* **3**, 95–101 (2007). <https://doi.org/10.1016/j.nano.2006.12.001>
- Chou, W.-L., Yu, D.-G., Yang, M.-C.: The preparation and characterization of silver-loading cellulose acetate hollow fiber membrane for water treatment. *Polym. Adv. Technol.* **16**, 600–607 (2005). <https://doi.org/10.1002/pat.630>
- Windler, L., Height, M., Nowack, B.: Comparative evaluation of antimicrobials for textile applications. *Environ. Int.* **53**, 62–73 (2013). <https://doi.org/10.1016/j.envint.2012.12.010>
- Arreche, R., Bellotti, N., Deyá, C., Vázquez, P.: Assessment of waterborne coatings formulated with sol-gel/Ag related to fungal growth resistance. *Prog. Org. Coat.* **108**, 36–43 (2017). <https://doi.org/10.1016/j.porgcoat.2017.04.007>
- Panacek, A., Kvitek, L., Prucek, R., Kolar, M., Vecerova, R., Pizurova, N., Sharma, V.K., Nevecna, T., Zboril, R., Kvi, L., Vec, R.: Silver colloid nanoparticles: synthesis, characterization, and their antibacterial activity. *J. Phys. Chem. B* **110**, 16248–16253 (2006). <https://doi.org/10.1021/jp063826h>
- Alvarado, R., Solera, F., Vega-Baudrit, J.: Síntesis Sonoquímica de nanopartículas de óxido de cinc y de plata estabilizadas con quitosano. Evaluación de su actividad antimicrobiana. *Revista Iberoamericana* **15**, 134–148 (2014)
- Brause, R., Möltgen, H., Kleineremanns, K.: Characterization of laser-ablated and chemically reduced silver colloids in aqueous solution by UV/VIS spectroscopy and STM/SEM microscopy. *Appl. Phys. B* **75**, 711–716 (2002). <https://doi.org/10.1007/s00340-002-1024-3>
- Mulvaney, P.: Surface plasmon spectroscopy of nanosized metal particles. *Langmuir* **12**, 788–800 (1996). <https://doi.org/10.1021/la9502711>
- Sosa, I.O., Noguez, C., Barrera, R.G.: Optical properties of metal nanoparticles with arbitrary shapes. *J. Phys. Chem. B* **107**, 6269–6275 (2003). <https://doi.org/10.1021/jp0274076>
- Zhao, Y., Jiang, Y., Fang, Y.: Spectroscopy property of Ag nanoparticles. *Spectrochim. Acta A* **65**, 1003–1006 (2006). <https://doi.org/10.1016/j.saa.2006.01.010>
- El Badawy, A.M., Luxton, T.P., Silva, R.G., Scheckel, K.G., Suidan, M.T., Tolaymat, T.M.: Impact of environmental conditions (pH, ionic strength, and electrolyte type) on the surface charge and aggregation of silver nanoparticles suspensions. *Environ. Sci. Technol.* **44**, 1260–1266 (2010). <https://doi.org/10.1021/es902240k>
- Cosgrove, T.: *Colloid Science: Principles, Methods and Applications*. Wiley, New York (2005). <https://doi.org/10.1097/0000433-198206000-00020>
- El-Zahry, M.R., Mahmoud, A., Refaat, I.H., Mohamed, H.A., Bohlmann, H., Lendl, B.: Antibacterial effect of various shapes of silver nanoparticles monitored by SERS. *Talanta* **138**, 183–189 (2015). <https://doi.org/10.1016/j.talanta.2015.02.022>
- Bastos, D.H.M., Ishimoto, E.Y., Ortiz, M., Marques, M., Fernando Ferri, A., Torres, E.A.F.S.: Essential oil and antioxidant activity of green mate and mate tea (*Ilex paraguariensis*) infusions. *J. Food*



- Compos. Anal. **19**, 538–543 (2006). <https://doi.org/10.1016/j.jfca.2005.03.002>
33. Berte, K.A., Beux, M.R., Spada, P.K., Salvador, M., Hoffmann-Ribani, R.: Chemical composition and antioxidant activity of yerba-mate (*Ilex paraguariensis* A.St.-Hil., Aquifoliaceae) extract as obtained by spray drying. J. Agric. Food Chem. **59**, 5523–5527 (2011). <https://doi.org/10.1021/jf2008343>
34. Bastos, D.H.M., Saldanha, L.A., Catharino, R.R., Sawaya, A.C.H.F., Cunha, I.B.S., Carvalho, P.O., Eberlin, M.N.: Phenolic antioxidants identified by ESI-MS from yerba mate (*Ilex paraguariensis*) and green tea (*Camellia sinensis*) extracts. Molecules **12**, 423–432 (2007)
35. Isolabella, S., Cogoi, L., López, P., Anesini, C., Ferraro, G., Filip, R.: Study of the bioactive compounds variation during yerba mate (*Ilex paraguariensis*) processing. Food Chem. **122**, 695–699 (2010). <https://doi.org/10.1016/j.foodchem.2010.03.039>
36. Anbinder, P.S., Deladino, L., Navarro, A.S., Amalvy, J.I., Martino, M.N.: Yerba mate extract encapsulation with alginate and chitosan systems: interactions between active compound encapsulation polymers. J Encapsul. Adsorpt. Sci. **2011**, 80–87 (2011). <https://doi.org/10.4236/jjeas.2011.14011>
37. Taylor, P., Marcelo, M.C.A., Pozebon, D., Ferrão, M.F.: Authentication of yerba mate according to the country of origin by using Fourier transform infrared (FTIR) associated with chemometrics. Food Addit. Contam. A (2015). <https://doi.org/10.1080/19440049.2015.1050702>
38. Shamailla, S., Sajjad, A.K.L., Ryma, N.A., Farooqi, S.A., Jabeen, N., Majeed, S., Farooq, I.: Advancements in nanoparticle fabrication by hazard free eco-friendly green routes. Appl. Mater. Today. **5**, 150–199 (2016). <https://doi.org/10.1016/j.apmt.2016.09.009>
39. Castro, L., Blazquez, M.L., Munoz, J.A., Gonzalez, F., Garcia-Balboa, C., Ballester, A.: Biosynthesis of gold nanowires using sugar beet pulp. Process Biochem. **46**, 1076–1082 (2011). <https://doi.org/10.1016/j.procbio.2011.01.025>
40. Buszewski, B., Railean-plugaru, V., Szultka-mlynska, M., Golinska, P.: Antimicrobial activity of biosilver nanoparticles produced by a novel *Streptacidiphilus durhamensis* strain. J. Microbiol. Immunol. Infect. (2016). <https://doi.org/10.1016/j.jmii.2016.03.002>
41. Dhand, V., Soumya, L., Bharadwaj, S., Chakra, S., Bhatt, D., Sreedhar, B.: Green synthesis of silver nanoparticles using *Coffea arabica* seed extract and its antibacterial activity. Mater. Sci. Eng. C (2015). <https://doi.org/10.1016/j.msec.2015.08.018>
42. Rasulov, B., Rustamova, N., Yili, A., Zhao, H.: Synthesis of silver nanoparticles on the basis of low and high molar mass exopolysaccharides of *Bradyrhizobium japonicum* 36 and its antimicrobial activity against some pathogens. Folia Microbiol. **61**, 283–293 (2015). <https://doi.org/10.1007/s12223-015-0436-5>
43. Agnihotri, S., Mukherji, S., Mukherji, S.: Size-controlled silver nanoparticles synthesized over the range 5–100 nm using the same protocol and their antibacterial efficacy. RSC Adv. **4**, 3974–3983 (2014). <https://doi.org/10.1039/c3ra44507k>
44. Ibrahim, H.M.M.: Green synthesis and characterization of silver nanoparticles using banana peel extract and their antimicrobial activity against representative microorganisms. J. Radiat. Res. Appl. Sci. **8**, 265–275 (2015). <https://doi.org/10.1016/j.jrras.2015.01.007>
45. Krishnaraj, C., Jagan, E.G., Rajasekar, S., Selvakumar, P., Kalai-chelvan, P.T., Mohan, N.: Synthesis of silver nanoparticles using *Acalypha indica* leaf extracts and its antibacterial activity against water borne pathogens. Colloids Surf. B **76**, 50–56 (2010). <https://doi.org/10.1016/j.colsurfb.2009.10.008>